ARC ROOTS FEM MODELLING AND SIMULATION AT PLANE ELECTRODES

J.M. Bueno Barrachina[(1)], S. Catalán Izquierdo [(2)], C.S. Cañas Peñuelas[(3)], F. Cavallé Sesé[(4)]

Instituto de Tecnología Eléctrica[(1)],
Avda. Juan de la Cierva, 24 - Parque Tecnológico de Valencia - 46980 Paterna (Valencia) - España,
jmanuel.bueno@ite.es
Instituto de Tecnología Eléctrica[(2,3,4)],
Avda. Juan de la Cierva, 24 - Parque Tecnológico de Valencia - 46980 Paterna (Valencia) - España,
saturnino.catalan@ite.es [(2)], cesar.canas@ite.es [(3)], fcavalle@ite.upv.es[(4)]

Abstract: **The aim of this work is to model and to simulate the arc root generation processes in plane electrodes using a three-dimensional solid model based on the finite elements method (FEM). For this purpose, a loop integrating an electrical model in transient state and a solid model constituted by two plane electrodes has been used. The model includes: current, voltage, circuit impedance, plasma parameters, current density and temperature.**
The simulation results show that local heating is non-significant at the electrode surface, hence uniform flows of current are obtained and a plasma column is generated without the appearance of intense metal-melting arc roots. These are steps into a more comprehensive fluid-thermo-electrical model of the arc using 3D FEM aimed at the development of more precise design and analysis engineering tools of arc based protection elements.

Keywords: **current limitation, arcs in air, arcing phenomena, electric arc.**

1. Introduction

The electrical arc can be defined as an independent discharge able by itself to generate the amount of ions and electrons necessary for the circulation of current. In these conditions some electrons have sufficient energy to cause the dielectric and thermal rupture of the insulating material that there is between the contacts (air in most of the current breakers).

The homogeneous and isotropic characteristics considered as well as the non-existence of macroscopic imperfections at the surface and inside the electrical contact (plane electrodes) causes that, even when distance between contacts is very small, the separation is uniformly constant along the surface hence, current concentration can not occur nor hot spots and arc roots.

The models developed in this paper study some of the thermal-electrical processes that take place in the electrical contacts and in the air when opening an electrical circuit.

2. Simulation

The model is formed by two contacts of cylindrical form Fig 1 and the air between them.

The process is started with the circuit in normal steady state operation. Next a short-circuit is introduced and the separation of the electrodes is started.

The implemented system allow to obtain [1] the initial current and voltage conditions, and, inside the 3D model, the transient arc voltage, current density and temperature distribution. The physical properties of high temperature air is taken from [2].

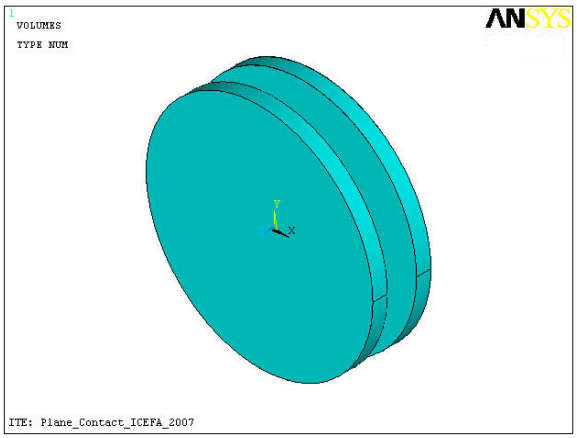

Fig. 1: Plane copper electrodes of a circuit breaker.

2.1. Heat Balance

The power balance equation for each volume element dV in the integral formulation is shown in equation 1. This equation is the balance between the

978-2-84516-363-8/07/$25.00 © 2007
Blaise Pascal Academic Press

heat stored by temporal change of temperature, the power removed from the element by thermal conduction and the heating power from the current flow [3]. In this model is not yet considered fluid mass transport.

$$\frac{j^2}{\sigma} = \rho \cdot C_p \cdot \frac{\partial T}{\partial t} - div(\lambda \cdot \nabla T) \qquad (1)$$

Where:

$\frac{j^2}{\sigma}$ = Joule heating

$\rho \cdot C_p \cdot \frac{\partial T}{\partial t}$ = Heat storage

$div(\lambda \cdot \nabla T)$ = Thermal conduction

j = Current density

σ = Electrical conductivity

ρ = Mass density

C_p = Specific heat at constant pressure

T = Absolute temperature

t = Time

λ = Thermal conductivity

∇T = Thermal gradient

2.2. Current density and Electric potential

The current density j necessary in equation 1 follows from

$$j_x = \sigma \partial U / \partial x \qquad j_y = \sigma \partial U / \partial y \qquad j_z = \sigma \partial U / \partial z$$
$$j = \sqrt{j_x^2 + j_y^2 + j_z^2} \qquad (2)$$

Where U is the electric potential, that follows the Laplace equation:

$$div(\nabla U) = 0 \qquad (3)$$

The current density j and the electric potential U must also satisfy the external circuit equation:

$$e(t) = L\frac{di}{dt} + Ri + U \qquad (4)$$

Where e(t), L and R are the external circuit characteristics, and U is the anode potential minus the cathode potential.

3. Materials and Methods

The simulation is started with the electrical model in sine stationary regime as in Fig 2.

This electrical model is constituted by a sine voltage generator (50 Hz) (1), the line impedance upwards from the arcing element (2), the two contacts equivalent resistors (3) and the line and load equivalent impedance downwards from it (4).

The voltage of the sine generator is 230Vrms, the line impedances have been calculated to obtain a current of 630 Arms with a very resistive power factor.

In time = 0.02 seconds a short circuit is introduced just downwards from the protective element. Fig. 3 shows the electrical circuit used to model this new condition.

The current of the circuit increases until the tripping level of the protective element, almost 880 amperes.

The electrical model to use in this condition is shown in Fig. 4.

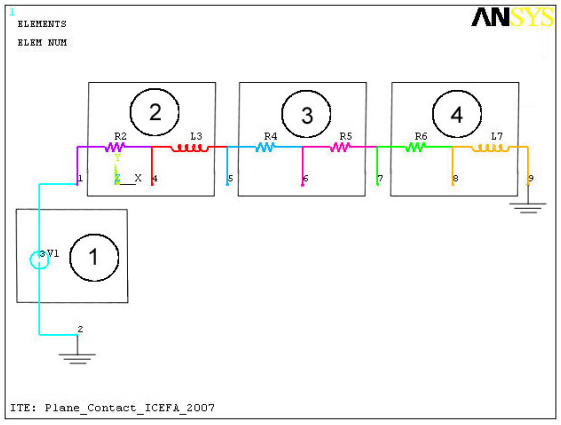

Fig. 2: Initial, steady state, electrical model.

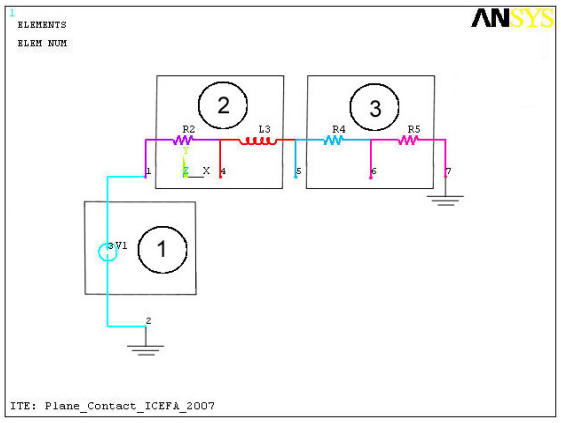

Fig. 3: Electrical model in short circuit.

978-2-84516-363-8/07/$25.00 © 2007
Blaise Pascal Academic Press

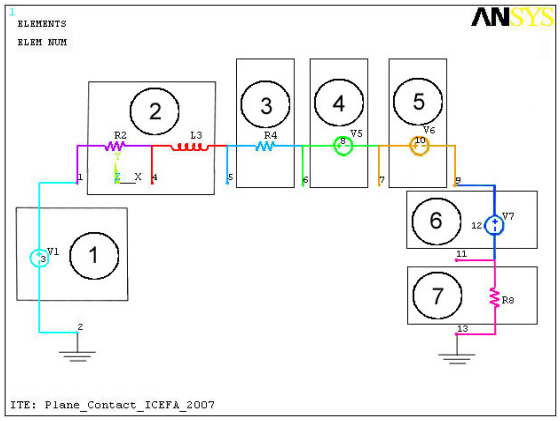

Fig. 4: Electrical model while contacts are opening.

The new electrical model is formed by a sine voltage generator (1), the line impedance upwards the element (2), the anode equivalent resistor (3), the voltage of the anode sheath (4), the plasma column voltage (5) , the voltage of the cathode sheath (6), and the cathode equivalent resistor of the element (7).

As a first approximation, constant voltage anode and cathode sheath have been considered.

The air between electrodes is, at first, relatively cold and therefore its resistivity is very high. This causes that voltage drop between electrodes increases. This affects the electric field increasing it.

At the same time, following equation 1, the temperature of the air between contacts increases. This causes that the resistivity of the air diminishes, and therefore the voltage drop between electrodes also diminishes, which causes that the electric field diminishes.

The combined effect of voltage drop, current and temperature cause the voltage drop to reach a balance at plasma air temperature.

In addition, it is also necessary to consider the increasing separation between electrodes that increases voltage drop forcing current to finally extinguish.

The plasma column and the electrodes have been modelled as pure resistive [4], this 3D model, based on the use of the method of the finite elements (FEM), has been generated with ANSYS® [5]. The FEM model in each iteration receives the electrical current and temperature at each node from the previous iteration and calculates the drop potential between the electrodes and the new distribution of temperature. At the same time the model separates the electrodes at a prefixed speed. The new electrical current for the next iteration is calculated by the electrical model circuit.

Provided that electrode surface is considered ideal and that no fluid analysis has been yet included, no radial motion is obtained. It has been chosen, as a first approximation, to situate the arc in the middle of the electrode surface.

Fig. 5 shows the 3D model used. This model is constituted by three volumes, first is the metallic electrode of the cathode (1), second is the sheath and the arc cathodic root (2) and third is the electrical arc (3).

In this analysis electric copper contacts have been modelled.

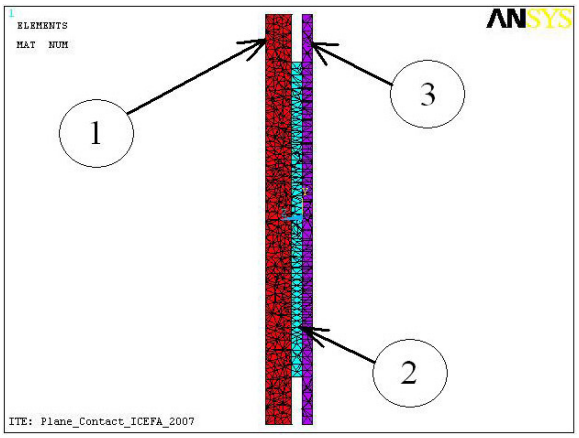

Fig. 5: Model at time = 20.527 ms.

4. Results

The simulation results show that local heating is non-significant at the electrode surface, hence uniform flows of current are obtained and the plasma column is generated without the appearance of intense metal-melting arc roots.

Fig. 6, 7, 8 show temperature, voltage and current density obtained in ANSYS® for the 3D model at several steps of the simulation.

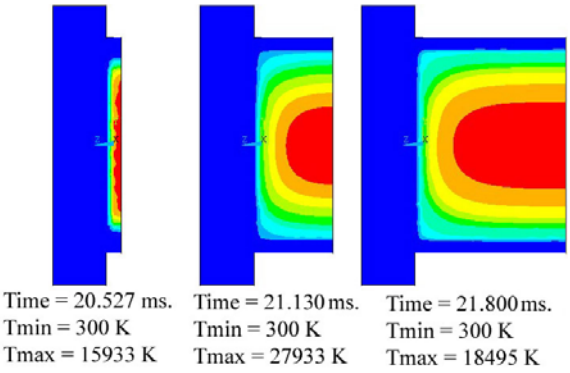

Fig. 6: Temperature distribution for the model at several steps of the simulation.

978-2-84516-363-8/07/$25.00 © 2007
Blaise Pascal Academic Press

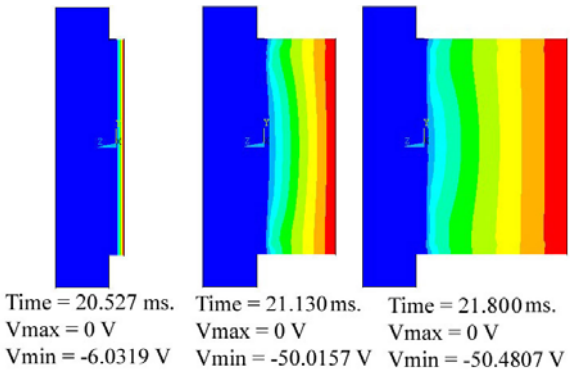

Fig. 7: Voltage distribution for the model at several steps of the simulation.

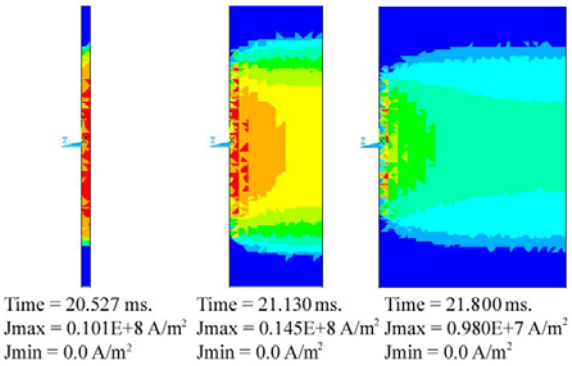

Fig. 8: Current density distribution for the model at several steps of the simulation.

Fig. 9 shows the simulation diagram used for this FEM model.

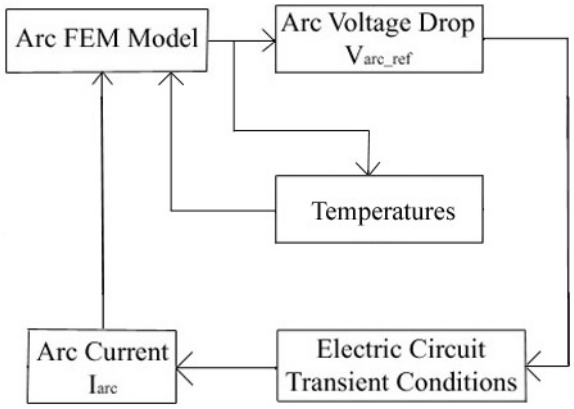

Fig. 9: Process diagram used in the simulation.

At the first step of the simulation the electric current obtained from the electric circuit show in figure 3 is applied to the 3D arc FEM model. Using this 3D model the voltage drop between electrodes is obtained by a transient analysis. This voltage drop is applied into the electric circuit shown in figure 4 and the transient analysis solution obtained from this circuit is the new input current to the arc FEM model.

A summary of the results obtained for arc voltage and current from the simulation is shown in Fig. 10. In this figure is presented part of the transient electric analysis (from 20.30 ms to 20.46 ms) just before the beginning of the aperture of the contacts. At 20.46 ms the electric arc process is started.

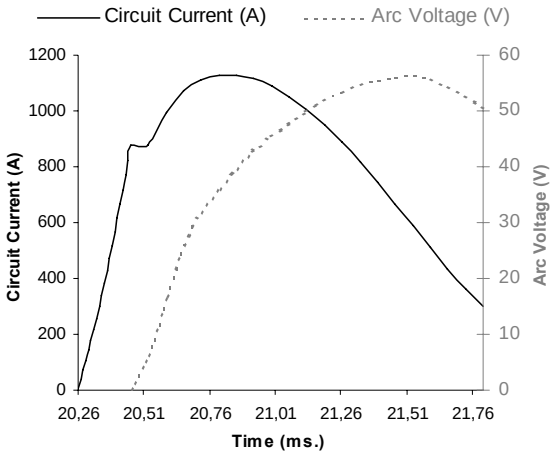

Fig. 10: Current and arc voltage waveforms.

Greater voltages do not appear at the first moments [1,4] because, as a first approximation, the initial plasma condition of the air is obtained by heating a small area of air between the contacts only in the first separation step.

Fig. 11 shows the temperature distribution as a function of the radius. The plasma column consists mainly of two zones: a low temperature area (LTA) between [300, 5000] K, and a high temperature area (HTA) in the range [10000, 20000] K. Most of the current is obtained from the HTA. It can be observed that there is a relatively small area between LTA and HTA in which the temperature changes abruptly.

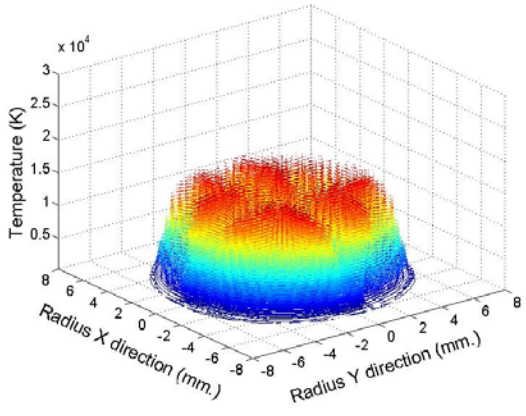

Fig. 11: Calculated temperature distribution along the radius at the centre of the arc in the first step of the simulation (time = 20.527 ms).

978-2-84516-363-8/07/$25.00 © 2007
Blaise Pascal Academic Press

Fig. 12 and 13 show the temperature distribution from the centre of the plasma column at several simulation steps.

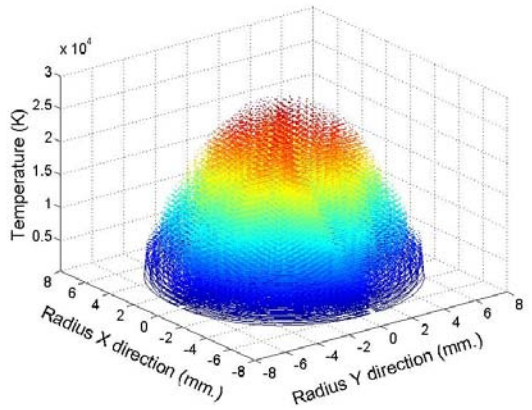

Fig. 12: Calculated temperature distribution along the radius at the centre of the plasma column (time = 21.13 ms).

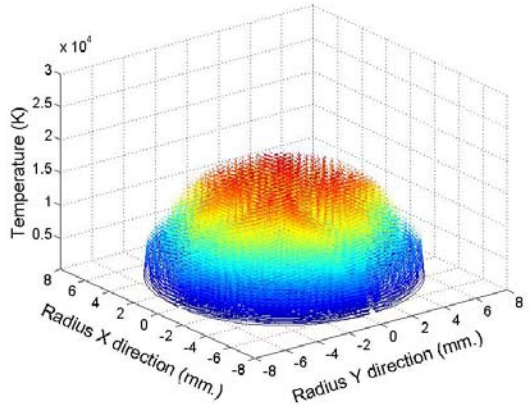

Fig. 13: Calculated temperature distribution along the radius at the centre of the plasma column in the last step of the simulation (time = 21.8 ms).

The obtained distribution agrees quite well with other published results [4].

5. Conclusions

The simulation results show that local heating is non-significant at the electrode surface, hence uniform flows of current are obtained and the plasma column is generated without the appearance of intense metal-melting arc roots.

The obtained arc consists mainly of two zones: a low temperature area (LTA) between [300, 5000] K, and a high temperature area (HTA) in the range [10000, 20000] K separated by a thin layer where temperature changes abruptly. Most of the current flows through the HTA.

These are steps into a more comprehensive fluid-thermo-electrical model of the arc using 3D FEM aimed at the development of more precise design and analysis engineering tools of arc based protection elements.

References

[1] M. Lindmayer, "The process of arc splitting between metalplates in low voltage arc chutes", IEEE Trans. Comp., Packag., Manufact. Technol. A, vol. 29, no. 2,pp. 310-317, June 2006.

[2] M. Capitelli, G. Colonna, C. Gorse and A. D'Angola, "Transport properties of high temperature air in local thermodynamic equilibrium", Eur. Phys. J. D, vol. 11, pp. 279-289, 2000.

[3] M. Lindmayer, "3D simulation of fusing characteristics including the "M-EFFECT"", *Proc. of the 6th ICEFA*, *Torino (Italy), Sept. 1999*, pp. 13-20.

[4] C. Lüders, T. Suwanasri and R. Dommerque, "Investigation of an SF_6 – selfblast circuit breaker", J. Phys. D: Appl. Phys, vol. 39, pp. 666-672, 2006.

[5] ANSYS® 9.0, User Documentation.

978-2-84516-363-8/07/$25.00 © 2007
Blaise Pascal Academic Press